Seasonal and longer-term variations in middle atmosphere temperature from HALOE on UARS

Ellis E. Remsberg
Atmospheric Sciences Research, Langley Research Center, Hampton, Virginia, USA

Praful P. Bhatt
Science Applications International Corporation, Hampton, Virginia, USA

Lance E. Deaver
Atmospheric Sciences Research, Langley Research Center, Hampton, Virginia, USA

Received 5 October 2001; revised 12 February 2002; accepted 13 February 2002; published 15 October 2002.

[1] The 9.5-year temperature time series from the Halogen Occultation Experiment (HALOE) aboard the Upper Atmosphere Research Satellite (UARS) has been analyzed for 40°N, 30°N, 20°N, Tropics, 20°S, 30°S, and 40°S using multiple linear regression techniques at 12 pressure levels from 5 to 0.01 hPa. The HALOE sunset and sunrise temperature profiles have good vertical resolution and are representative of the variations of the zonal average state. Vertical profiles with latitude of the average sunset/sunrise differences agree qualitatively with that expected from the effects of tides. Periodic seasonal (annual and semiannual) terms are sampled well in the time series, and the seasonal cycle from HALOE at 40°N agrees well with the local variations reported from measurements with the ground-based Rayleigh lidar instrument at 44°N, 6°E. Significant quasi-biennial oscillation (QBO)-like variations occur at most latitudes of the upper stratosphere in the HALOE data, and their phases are nearly symmetric about the equator. There is also a clear subbiennial (688-day) cycle at Northern Hemisphere (NH) midlatitudes at those same pressure altitudes due to the interaction of the QBO and annual cycles. The solar cycle temperature term is in-phase with the UV flux forcing in the upper stratosphere but lags it by a year or so in the upper mesosphere at NH midlatitudes. There is also a significant cooling trend for the HALOE time series that is of order 1.0 to 1.6 K per decade in the midmesosphere at 20°N and at 1 hPa in the tropics. The seasonal terms may be combined with the constant and autoregressive (AR) terms (or annual average distribution that we provided) in order to generate the monthly zonal average HALOE "climatology" of middle atmosphere temperature for the decade of the 1990s. Comparisons between the HALOE and CIRA climatologies for the upper stratosphere suggest a cooling of order 2.5 K per decade from the mid-1970s to the mid-1990s. HALOE/CIRA differences for the mesosphere change sign with altitude, an indication of bias errors in one or both. *INDEX TERMS:* 0340 Atmospheric Composition and Structure: Middle atmosphere—composition and chemistry; 0350 Atmospheric Composition and Structure: Pressure, density, and temperature; *KEYWORDS:* temperature climatology, middle atmosphere, satellite observations, regression analysis

Citation: Remsberg, E. E., P. P. Bhatt, and L. E. Deaver, Seasonal and longer-term variations in middle atmosphere temperature from HALOE on UARS, *J. Geophys. Res.*, *107*(D19), 4411, doi:10.1029/2001JD001366, 2002.

1. Introduction

[2] Both global and local data sets are being used for the determination of seasonal and interannual changes of middle atmosphere temperature, as well as its trends due to increases in the so-called greenhouse gases [*World Meteorological Organization*, Chapter 5, 1999; *Randel et al.*, 2000; *Ramaswamy et al.*, 2001]. For example, since 1979 the Stratospheric Sounding Unit (SSU) and Microwave Sounding Unit (MSU) instruments on operational meteorological satellites have yielded daily global observations of temperature up to ~55 km. They also provide daily zonal mean brightness temperatures (i.e., radiances) but at a vertical resolution of only 8–15 km. To determine significant trends, one must remove structure from the time series by accounting for the periodic seasonal and interannual terms plus the effects of external forcings, such as a solar cycle or a volcanic perturbation. But because the series of SSU and MSU instruments lack an onboard absolute

Copyright 2002 by the American Geophysical Union.
0148-0227/02/2001JD001366

calibration and make their observations at local solar times that vary for successive satellites, it has been difficult to make the necessary adjustments for connecting those multiple records into a single time series, especially for the decade of the 1990s [*Finger et al.*, 1993; *Keckhut et al.*, 2001]. Nevertheless, these long-term, global data sets are the basis of the stratospheric temperature climatology, its periodic variations and trends [e.g., *Scaife et al.*, 2000].

[3] Radiosonde observations provide the longest temperature record at and below the 10-hPa level (near 30 km) at both 00Z and 12Z [*World Meteorological Organization*, 1999]. While their bead thermistors are well-calibrated, their temperature records require significant radiative corrections for the 10-hPa to 30-hPa levels [*Gaffen*, 1994; *Remsberg et al.*, 1992]. Temperature time series have also been obtained from several stations of the meteorological rocketsonde network from 25 to ~55 km with a tabulated vertical resolution of 1 km [*Keckhut et al.*, 1999]. Those rocket time series indicate a cooling in the upper stratosphere and lower mesosphere of order 1.7 to 3.3 K per decade from the late 1960s to the early 1990s [*Dunkerton et al.*, 1998; *Keckhut et al.*, 1999]. Local time series are also available from ~30 km to nearly 85 km with a vertical resolution of 1 to 3 km from ground-based Rayleigh lidar at 44°N, 6°E [*Keckhut et al.*, 1995]. Trends from the lidar indicate a cooling in the range of 0.8 K (5 hPa) to 3.1 K (0.4 hPa) per decade over the period 1979 to 1993 [*Keckhut et al.*, 2001]. Those cooling trends may have been dominated by the significant decline in the upper stratospheric ozone and its radiative heating effects during those years [*World Meteorological Organization*, 1999]. A primary concern with the rocket and lidar station observations is that they may not be representative of the periodic variations of the zonal mean, especially during the winter. As with the satellite temperatures, one must also consider the effects of temperature tides in time series analyses for their periodic and trend terms. Accordingly, *Luebken* [2000] concludes, on the basis of a combination of rocket grenade and falling sphere measurements, that there has been almost no cooling from 1964 to 1996 throughout the polar summer mesosphere where the effects of tides and planetary wave activity are less important.

[4] Satellite data have also been used to generate monthly "temperature climatologies." For example, the COSPAR International Reference Atmosphere (CIRA) model for middle atmosphere temperature is based on 3 years of data from the Pressure Modulated Radiometer (PMR) of Nimbus 6 plus 2 years of data from the Selective Chopper Radiometer (SCR) of Nimbus 5 for the mid-1970s [*Fleming et al.*, 1990]. Both instruments are nadir-viewing radiometers with their attendant low vertical resolutions. *Clancy et al.* [1994] have provided higher-resolution, near-global temperatures versus altitude from 40 to 92 km from 4 years of Solar Mesosphere Explorer (SME) satellite data of the mid-1980s. Both data sets were obtained from polar orbiting satellites that made their measurements at one or two local solar times. Neither data set is truly representative of the solar cycle period or possible decadal-scale changes on the net circulation of the middle atmosphere.

[5] In this paper we examine the middle atmosphere temperature time series on pressure surfaces (or $T(p)$), as obtained with the Upper Atmosphere Research Satellite (UARS) Halogen Occultation Experiment (HALOE) instrument from October 1991 through April 2001, 9.5 years. Our goal is to provide the seasonal and longer-period changes in $T(p)$ from 5 to 0.01 hPa based on nearly a decade of data. Although the HALOE measurements are not obtained at the same latitudes each day because of the geometry of solar occultation measurements constrained by the satellite orbit, up to 15 sunrise (SR) and 15 sunset (SS) measurements occur with a near-monthly frequency at low and middle latitudes. As a result, the HALOE profiles are representative of the zonal variations for SR and for SS for the dates of its measurements, and they are obtained often enough (on an average of every 17 days) to define the seasonal cycles in atmospheric temperature. Shorter-period changes, such as from a stratospheric warming, cannot be characterized well because of the much longer revisit times for the HALOE sampling at high latitudes.

[6] The measurements for our HALOE time series occurred at nearly uniform intervals and provided representative zonal average data over the span of 9.5 years. Such consistent sampling for each latitude zone sharply reduces the uncertainties in the seasonal cycle caused by the lack of daily occultation data. Multiple linear regression (MLR) analysis techniques were then used to determine the significant periodic and polynomial terms in the HALOE time series. We conducted analyses for 10° wide middle latitude zones of both hemispheres and for 12 levels from 5 to 0.01 hPa. Poleward of ~45° latitude, there are much larger data gaps from mid-1997 onward, reducing the accuracy of the seasonal cycles that we can obtain; we do not report results for those higher latitudes. Temperature time series were also analyzed for a single, wide tropical latitude zone of 15°S to 15°N, where the effects of the quasi-biennial oscillation (QBO) are most direct at least for the middle stratosphere. The HALOE record is long enough to resolve 4 QBO cycles and nearly a solar cycle. We analyzed for this set of terms with the MLR model and then tested its residual for any remaining significant trend terms. The justification for our approach is discussed further, and the results from our analyses are presented in the following sections. Initially we focused our analysis at 40°N (see section 4), where similar results have been reported from local ground-based sounding sites. In section 5 we discuss our findings for other latitudes. HALOE temperatures are also compared in section 6 with the CIRA model and with seasonal variations from lidar.

2. Quality of HALOE Temperatures

[7] HALOE is a limb-viewing solar occultation experiment and obtains transmittance profiles in the 2.8-micrometer band of CO_2 and at two fixed local solar times, SR and SS [*Russell et al.*, 1993]. These radiometer channel measurements are essentially "self-calibrated" because they are referenced to exoatmospheric solar intensities for each scan. Other calibration measurements have been taken at intervals throughout the mission life of HALOE to check for linearity, effects of optical misalignment, and changes in solar tracking accuracy. The 2.8-micrometer filter characteristics have been stable, based on lifetime test measurements of the witness filters in the laboratory and on related onboard measurements. The range of possible measurement and retrieval errors that could affect the HALOE trends in

$T(p)$ and ozone were described by *Harris et al.* [1998], but no problems have been found. Steady adjustments have been made for the known, nearly linear, 0.47% per year trend in the CO_2 mixing ratio of the troposphere, as part of the algorithm for the pressure registration of the HALOE transmittance profiles. Further, studies have been performed to evaluate the effects of changes in HALOE sampling on its ability to provide accurate seasonal cycles and trends both globally and in latitude zones, and those effects are negligible for the latitude zones of this study [J. Russell and J. Anderson, personal communication, 2000].

[8] HALOE temperature profiles are retrieved from its CO_2 channel transmittances with a vertical resolution of ~4 km from ~0.01 hPa to near the 10-hPa level. However, because the accuracy of the forward model is degraded near 10 hPa, the HALOE algorithm uses temperatures below the 5-hPa level from the National Center for Environmental Prediction (NCEP) analyses that were provided to the UARS project office. There is good agreement between the HALOE and NCEP results in their altitude region of overlap (35 to ~40 km). At this point we note that the NCEP analyses through most of the UARS period were obtained from the SSU sensor on NOAA 11, and we did not expect that our midstratosphere time series would be affected by any discontinuities arising from our tie-on to the NCEP data. We were reassured when we found no such problem in the plot of the residual from our MLR model fit to the data at 5 hPa.

[9] *Hervig et al.* [1996] show correlative comparisons and error estimates for the HALOE Version 17 (V17) temperatures, and their results show good agreement. The present HALOE Version 19 (V19) data set employs improvements in the pressure registration of the profiles and corrects the discontinuity in the vertical resolution of the V17 profiles near 60 km. As a result, the HALOE V19 temperatures compare better with the correlative lidar and inflatable falling sphere measurements of the midmesosphere; those statistical comparisons are reported by *Remsberg et al.* [2002].

3. Data Analysis

[10] The HALOE V19 SR and SS $T(p)$ values from the ozone word block of the Level 2 files were interpolated onto a set of 12 pressure levels. Separate zonal averages were calculated for the individual SR and SS sweeps in 10° wide bins centered at 40°N, 30°N, 20°N, 20°S, 30°S, and 40°S. Each latitude bin is normally composed of several days of profiles. Hence, the exact date of each time series point is obtained by averaging the times of the individual profiles. We use a single 30° wide bin centered on the equator to represent variations for the entire tropical region. Narrower 10° bins do not have good zonal coverage in the tropics because the HALOE tangent track moves more rapidly across that region. Time series plots from 6 levels at 40°N are shown in Figure 1. The SR and SS temperature averages are indicated by open and solid circles, respectively. The mean values for the SR and the SS series were determined for a level, and an adjustment for half the difference of those means was applied in the generation of the SR and SS points for each level of Figure 1 and prior to the fitting of model terms to the combined series of 144 points.

[11] The time series analysis was conducted by employing MLR techniques. Terms in the model are given in equation (1).

$$T_n = a + bT_{n-1} + cX + dX^2 + e \sin(Z + \Phi) + \epsilon_n, \qquad (1)$$

where T_n is the temperature at the nth point in the time series, T_{n-1} represents the time series with a lag-1 or autoregressive term, and a, b, ... are the coefficients. The model includes linear and quadratic terms for $X = (\tau_n - \tau_1)/t$, where τ_n is the time of the nth observation point, τ_1 is the first point in the time series, and t is the total length of the time series. Linear and quadratic terms were seldom significant, however. For the periodic terms $Z = 2\pi\tau_n/P$, with P being their period and the coefficient e their amplitude. The variable Φ is the appropriate phase to account for the cosine component. ϵ_n is the residual. Autoregressive terms account for the fact that there is memory between the time series T_n and the same series lagged by one point, T_{n-1}, in part because the periodic model terms do not exactly fit the phase of every repeating cycle. The coefficient b is a dimensionless fraction, and the value of the AR-1 term can be approximated as $b\ T_{\mathrm{mean}}$, where T_{mean} is the average value over all the data in the series.

[12] A description of our approach and significance testing as applied to HALOE time series data is given for global average HF and HCl by *Considine et al.* [1999] and for zonal averages of lower stratospheric ozone in 10° latitude bins by *Remsberg et al.* [2001]. It is noted at this point that negative signs were assigned arbitrarily to the amplitudes of the periodic ozone terms in the tables of *Remsberg et al.* [2001], to indicate when the ozone maximum occurred in the second half of its period. In the present paper the coefficient e is always positive, and its maximum value is listed in days as referenced to the length of the period of each term. The analysis procedure that we used had several objectives. Each term had to exceed the 95% CI in both its rank-order correlation (ROC) and partial rank-order correlation coefficients in the manner of *Considine et al.* [1999] and *Remsberg et al.* [2001]. AR terms were required to meet that level of significance for only the ROC criterion. A Fourier analysis was used to identify interannual structure in the residual time series after accounting for the seasonal and AR terms. We tested models with the longer-period and polynomial terms that were indicated and finally chose the model that had the maximum number of terms with CI greater the 95%.

[13] Annual and semiannual oscillations (AO and SAO) define the seasonal terms. The period and phase of the quasi-biennial oscillation (QBO) varies with latitude, longitude, and altitude and at midlatitudes of the upper stratosphere may combine with the AO to yield a significant subbiennial cycle [*Dunkerton*, 2001]. Therefore, rather than simply including one interannual (IA) term based on the observed QBO wind cycles at selected tropical stations, we determined the atmospheric response to the QBO with one or more IA terms whose periods were indicated by an analysis of the Fourier modes of the time series of the residual after removal of the seasonal cycle. For instance, we found IA terms with periods of 688 days (22.6 months) and 800 days (26.3 months) at 30°S, 30°N, and 40°N. By

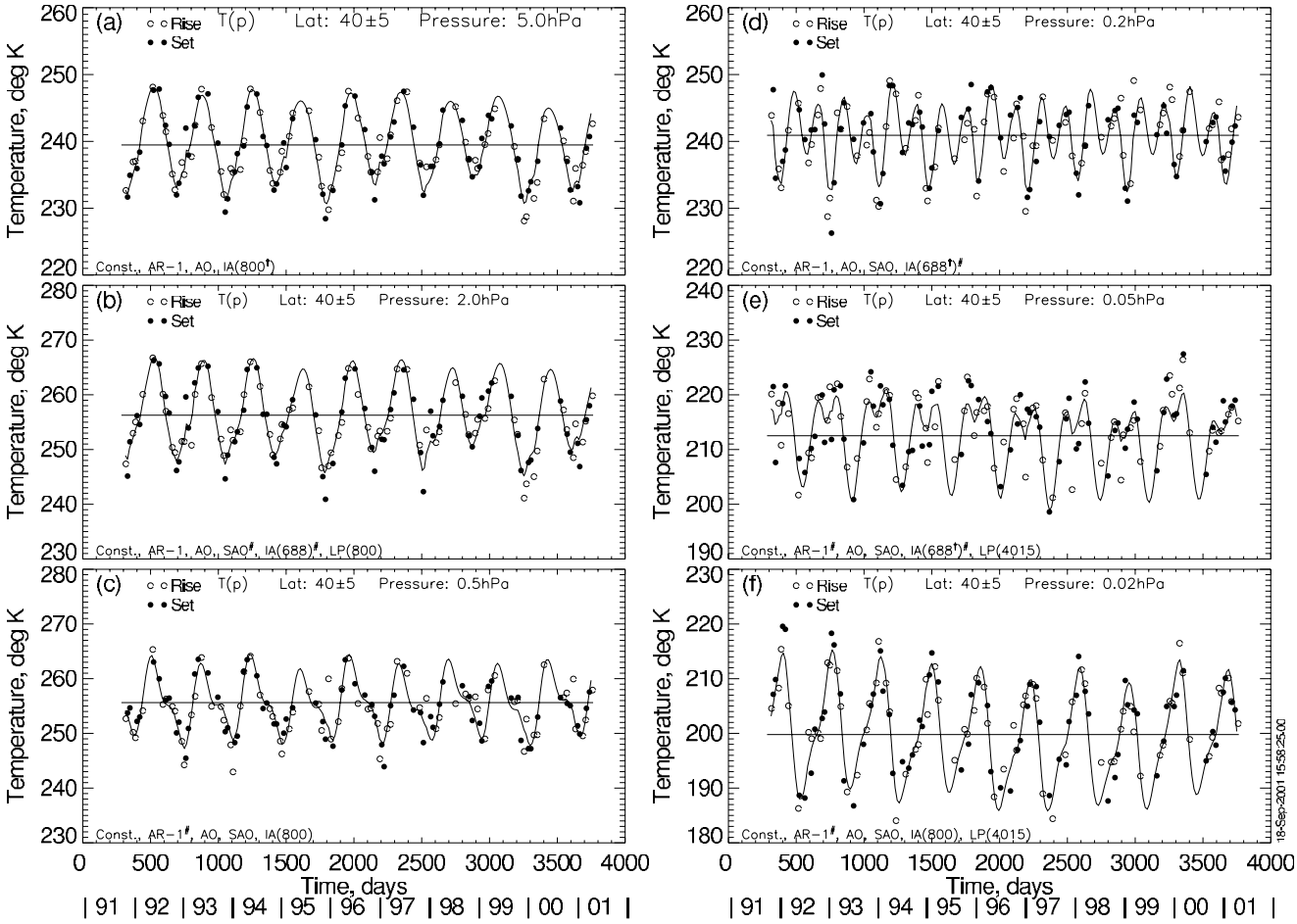

Figure 1. HALOE temperature time series; the sunrise (open circles) and sunset (solid circles) temperature zonal average points at 40°N for 6 pressure levels from 5 to 0.02 hPa. The model fit to the data (solid curve) is based on the model terms indicated at the bottom of each panel. The solid horizontal line in each panel is the sum of the terms a and b T_{mean}.

analyzing for IA terms in this manner, we were able to identify and account for almost all of the longer-period structure in our time series residual. Yet, this approach requires that separate MLR models be developed for each latitude zone and pressure level. We then looked for continuity in model terms at adjacent levels and latitudes in order to judge whether those terms were physically consistent. Our goal was to find model terms based on known atmospheric forcings, while at the same time requiring a threshold level of statistical significance for each of the terms and then the complete model.

[14] The MLR analysis routines also indicate whether there are any significant and unaccounted for lag-autocorrelation, linear trend, and/or uncharacterized long-period (LP) dynamical effects in the residual. First, autocorrelation in the time series residual was examined over a range of lag values, as depicted by *Remsberg et al.* [2001, Figures 4a, c and 5a, c]. There can be significant correlation at lag-1, primarily because successive atmospheric cycles do not have identical periods and amplitudes, and yet we have fit them with repeating AO, SAO, and IA terms over the 9.5-year time series. The AR-1 term also accounts for some of the model/data mismatch due to any unmodeled atmospheric cycles. A small coefficient for the AR-1 term indicates an excellent model fit to the data for all cycles in the time series or else that the data are noisy. Linear and quadratic terms were also considered. Note that a linear term may appear significant if an AR-1 term is not evaluated first, leading to a flawed model. We checked for any remaining structure in the residual in the manner of *Remsberg et al.* [2001, their Figures 4c versus 5c).

[15] The 27-day solar cycle can barely be resolved with the low frequency of HALOE observations for a latitude zone, and the theoretical amplitude of this solar cycle is only ≈0.25°K, according to *Brasseur* [1993], or of the order of the noise in the HALOE data series in the mesosphere. At several altitudes our Fourier analysis of the residual indicated a period of the length (3442 days) of the data set or longer. The obvious candidate is an external forcing due to the 11-year (4015-day) solar cycle. While the length of the data is shorter than that period, both direct and indirect effects from a solar cycle forcing have been tentatively established from both theory and observations, most notably near the stratopause [see *Ramaswamy et al.*, 2001, and references therein]. *Garcia et al.* [1984] and *Huang and Brasseur* [1993] have calculated the temperature response due to the 11-year changes in the

solar UV flux: solar max minus solar min. They show a relative maximum positive (warm) response near the stratopause and even larger positive values from just below the mesopause and extending into the lower thermosphere. Initially we regressed against the observed F10.7 cm solar flux, but that proxy term was insignificant at the 95% CI and is not present in our final models. Instead, we simply specified a periodic, 11-year solar cycle (SC) term and then allowed our MLR routines to fit it to the time series residual. Then we evaluated the significance and phase of that SC term.

4. Results for 40°N

[16] The individual model terms are given for 40°N in Table 1 for each of the 12 levels. Figure 1 is a plot of the HALOE temperature time series at selected levels between 5 and 0.02 hPa, as shown in Figures 1a through 1f. The SR and SS data points are represented as open and solid circles, respectively, after adjustment for the mean difference of SS minus SR. The periodic solid curve is the fit to the data from the model terms. The horizontal solid line indicates the polynomial terms (at 40°N just the constant term a plus an approximation for the autoregressive (AR) term or b T_{mean}). The adopted model terms for each of the pressure levels are indicated in the bottom part of the panel. Note that normally the LP term refers to the solar cycle period, but in Figure 1b for 2 hPa it denotes the second of two significant IA terms. The superscript "#" indicates that the term is significant at better than 95% confidence interval (CI) but less than 99% CI. Table 1 shows that the AO is dominant in the upper stratosphere and lower mesosphere and at the 0.05-hPa level and above. The SAO term has the larger amplitude in the midmesosphere. One can easily see that the regression models fit the data well in Figure 1 and that the AO and SAO terms vary with altitude. One interesting aspect of the time series is that there is very little scatter in the points at temperature maxima, which occur in summer for panels (a) through (c). There is much more scatter near temperature minima, which occur in response to when there are winter warmings at higher latitudes. The associated meridional temperature gradients can change within weeks. In Figure 1f for 0.02 hPa the temperature maximum occurs during midwinter. Nevertheless, the MLR model fits through the wintertime values well in each panel. The larger scatter in the data at 0.05 hPa is due, most likely, to the random-like effects of breaking gravity waves on the temperature and mean meridional circulation (see section 4.3). Table 1 shows that the SAO term is absent at 5 hPa, indicating that while SAO forcings may be present, their amplitudes are not large enough to be highly significant.

[17] Table 1 contains a summary of the coefficients for the model terms for each pressure level, and we discuss them in the following subsections. Column 2 contains the mean SS minus SR differences in degrees K, which we relate to the strength of the tidal components that affect the separate SS and SR time series. The time series mean T_{mean} is in column 3. Column 4 is the constant value a, and column 5 is the coefficient b of the AR-1 term of the MLR model. Next we show the amplitudes of the AO and the SAO terms in degrees K in columns 6 and 7. The amplitudes of the 688-day (asterisk) and 800-day IA terms are given in column 8. The amplitude of the 4015-day SC term is in column 9.

Table 1. HALOE Zonal Mean Temperature Model for 40N[a]

P, hPa	SS-SR, K	Mean, K	a, K	b	AO, K	SAO, K	IA,[b] K	SC, K
5.0	−0.3	238.4	150.6	0.373	4.5	–	0.8	–
3.0	1.0	247.5	176.9	0.291	5.9	0.8	*0.7/0.9	–
2.0	2.7	254.8	178.1	0.307	6.1	1.0	*0.7/0.9	–
1.0	4.2	260.0	201.6	0.229	5.4	1.0	0.7	–
0.5	3.0	254.3	228.7	0.106	5.3	2.5	0.9	–
0.3	1.2	247.3	193.0	0.223	3.4	3.4	0.8	–
0.2	−0.4	240.7	187.0	0.224	1.6	4.4	*0.7	–
0.1	−2.5	227.5	189.8	0.162	2.0	5.0	*1.4	–
0.05	−1.8	214.5	177.6	0.163	6.1	4.0	*1.0	1.0
0.03	0.3	206.6	166.4	0.184	7.9	3.4	1.0	1.5
0.02	2.1	202.2	174.7	0.124	9.6	3.4	1.1	1.7
0.01	3.8	197.6	154.1	0.206	10.7	–	–	–

[a] Time series adjusted for SS/SR differences; series length is 3442 days.
[b] IA terms have periods of 688 (*) and/or 800 days.

4.1. SS/SR Differences

[18] *Keckhut et al.* [1996] and *Dudhia et al.* [1993] have analyzed Microwave Limb Sounder (MLS) and Improved Stratospheric and Mesospheric Sounder (ISAMS) data, respectively, over a 36 to 40 day UARS yaw cycle for Northern Hemisphere (NH) winter and determined the amplitudes and phases of both the diurnal and semidiurnal tides at 44°N. They showed a diurnal temperature maximum at NH midlatitudes near SS in the upper stratosphere. The semidiurnal tide, while not as well defined, had its daily maxima near SR and SS in the upper stratosphere, shifting closer to noon and midnight in the midmesosphere. *Hitchman and Leovy* [1985] approximated the diurnal temperature tide from a series of 216 daily averages from the Sun-synchronous Nimbus 7 Limb Infrared Monitor of the Stratosphere (LIMS) measurements taken at ∼1300 and 2300 LT. They also showed that the plot of phase versus altitude for those day/night differences remained nearly constant over the 216-day record in the tropics. At higher latitudes those estimated tidal amplitudes varied seasonally by less than a factor of two at most levels. They found a secondary tidal feature in the mesosphere near 40°N, where the semidiurnal tide can be important. The LIMS and the present HALOE measurements primarily sample the diurnal tide, which is expected to have its maximum amplitude at low latitudes.

[19] In the extratropics SS/SR differences are still expected because of diurnal tides, and we have consistently seen such differences in the average of pairings in longitude of HALOE SS and SR profiles for the so-called "crossover days." A crossover is when the intersections of the orbital SS and SR tangent track locations actually occur at the same latitude within the same day. At equinox, SS and SR are 12 hours apart, and the semidiurnal tide will not contribute to their difference. At solstice that separation time is not 12 hours, especially at the higher latitudes. There are also effects of breaking gravity waves in the local temperatures in the mid to upper mesosphere. Although the effects of tides are not as clear at midlatitudes, we still adjust our combined time series for the mean of SS/SR differences. This approach is helpful because merging both the SS and

SR data into a single time series doubles its sample size and enhances the statistical confidence of all the terms in the MLR model. Seasonal variations of the tides will affect our AO and SAO terms and their variances. However, when we did not make an adjustment for the mean SS/SR difference, the variances for the periodic model terms were greater and their significance was not as high.

[20] The daily temperature maximum for HALOE occurs at SS near 1 hPa at 40°N (see Table 1, column 2), and the SS-SR differences are positive between 3 and 0.3 hPa and at the 0.03-hPa level and above. The sign of the SS-SR differences is dictated by the phase of the hour of the maximum. Differences are greatest at 1 hPa and at 0.01 hPa, an implied vertical wavelength for tides of 32 km. The maximum values for the differences are similar to those reported from the ISAMS data [*Dudhia et al.*, 1993] and from the MLS data at 40°N, as well as from the lidar measurements of the Observatorie de Haute Provence (OHP) in France at 44°N, 6°E [*Keckhut et al.*, 1996]. At ~0.2 hPa the amplitude of the diurnal tide is expected to be near zero at SS and SR in agreement with our small mean differences at those levels [*Lindzen*, 1967; *Zhu et al.*, 1999]. Between 0.05 and 0.03 hPa the tidal oscillation continues to change such that the hour of maximum is near SS again and the SS-SR values are positive. Thus it is concluded that the HALOE results at 40°N are in accord with the tidal models.

4.2. AR-1 Term

[21] There is a fundamental restriction on statistical modeling of atmospheric variations that cannot be ignored, that is, the state of the atmosphere today depends on that of yesterday (memory). Also smoothly varying effects, such as slight mismatches in the amplitude or phase of the seasonal or IA terms, are handled in the MLR model by AR terms. This situation explains why an AR term can be significant for our time series even though the point spacings range from days to weeks and the radiative and chemical relaxation times in the mesosphere are short. If this intermediate-scale structure in our HALOE residual is ignored, its effects will alias into the longer-period and trend terms [*Considine et al.*, 1999; *Weatherhead et al.*, 1998]. The AR term is present at the 99% CI at all levels, although its coefficient is only ~0.2 in the mesosphere. The AR coefficient in Table 1 has its minimum value at 0.5 hPa, indicating that the AO and SAO cycles are very repeatable in the data at this level. There is an increase in the coefficient at 0.01 hPa, most likely because an SAO residual exists but is not highly significant and not in our model for this level. An AR-2 term is not highly significant, in general, and is not found in our final models, except at subtropical latitudes where some of the SS and SR points occurred only a day or two apart.

4.3. Seasonal Terms

[22] Table 1 contains the profile of the AO temperature amplitude, and this term is 99% significant at all levels. Each periodic term was estimated by the sine and cosine components fit to the data. The cosine component was accounted for by the phase variable (Φ) in the periodic sine term of equation (1). Because of the dominance of the AO forcing in temperature, its amplitude and phase are insensitive to the presence of the IA or other long period terms in the MLR model. The time of the AO maximum temperature (its phase relation) is given in Table 2 in days with pressure-altitude. That AO time of maximum is relatively constant (≈151–169 days) between 5 and 0.2 hPa, indicating that the warmest temperature occurs during late spring to summer. Then there is a rapid shift to a maximum in January from 0.1 hPa to the mesopause [cf. *Leblanc et al.*, 1998].

Table 2. Day of Maximum for Periodic Term

P, hPa	AO, 365[a]	SAO, 182.5[a]	IA, *688/800[a]	SC, 4015[a]
5.0	151	–	586	–
3.0	153	180	*191/540	–
2.0	154	180	*209/506	–
1.0	157	135	467	–
0.5	166	125	397	–
0.3	168	118	414	–
0.2	169	113	*554	–
0.1	1	108	*538	–
0.05	5	88	*523	836
0.03	9	67	135	682
0.02	12	52	135	564
0.01	10	–	–	–

[a] Assigned period in days.

[23] The SAO term is significant at 99% CI at nearly all levels, except at 5 hPa and 0.01 hPa where it has <95% CI. Its amplitude is in Table 1, and its time of temperature maximum is given in Table 2 in terms of the first 182.5 days of the year (first SAO cycle). That time gradually advances as the effects of the SAO descend. The interaction between the AO and SAO terms is evident in many of the data time series and our model fits to them are shown in the panels of Figure 1. We note here that the Fourier analysis routine often finds significant structure in the time series with a period of only 163 or 172 days, rather than 182 days, after accounting for the AO term. This shift to a shorter period is within the Nyquist frequency for our sample spacing and is not significant. There may also be interaction between the SAO cycle and some shorter period term. Still, a 182-day SAO model term accounts for that periodic structure in the time series residual. The SAO term dominates in the midmesosphere at 40°N. One can see in Figure 1d that the net effect of the AO and SAO terms yields a temperature amplitude that is larger for the first half of a year.

4.4. Interannual (IA) Term and the QBO

[24] *Wallace et al.* [1993] represented the effects of the QBO winds using empirical orthogonal functions (EOFs) to account for their amplitude and phase at a point over time. *Randel and Wu* [1996] incorporated EOFs with singular value decomposition (SVD) techniques to estimate the effects of the QBO forcing in ozone and NO_2. But *Huesmann and Hitchman* [2001] emphasize that the QBO amplitude, period, and phase vary from cycle to cycle and with latitude, longitude, and altitude. They have recommended a QBO-proxy based on the anomaly in the zonal mean wind shear at the equator.

[25] Our approach is empirical in that we applied Fourier analyses to the time series of the residual after accounting for the AR and seasonal (AO and SAO) terms. In the upper stratosphere two IA periods emerged as highly significant: 688 days and 800 days. We refer to the 800-day term as the nominal QBO-cycle from our HALOE time series. The 688-day term is the more significant one in the midmesosphere. These terms have about equal amplitude but are out-of-

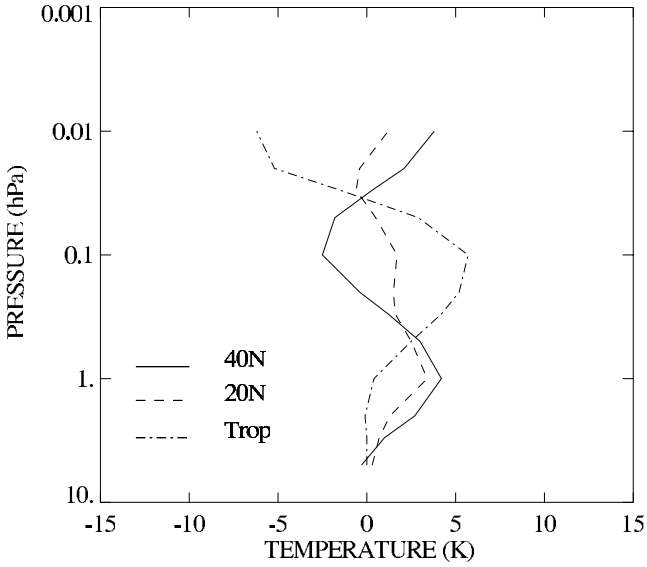

Figure 2. Average profiles of the HALOE sunset minus sunrise temperatures (K) for the 40°N, 20°N, and tropical zones.

phase (see Table 1, column 8, and Table 2, column 4). The 688-day (subbiennial) term is interpreted as evidence of an interaction between the AO and QBO, as calculated by *Dunkerton* [2001], and we note that both the 688- and 800-day terms are significant at 95% at 2 and 3 hPa. Separately, those terms are 95% significant at 5 hPa, too, but when both are included in our MLR model, the 688-day term has significance below 95%. The effects of the AO/QBO interaction are weaker at higher altitudes; the 800-day cycle emerges in the lower and upper mesosphere. Amplitudes of both IA terms are of order 0.8 K. Although we developed separate MLR models for each of our pressure-altitudes, the continuity in the time of maximum with altitude implies that our empirical IA terms are physically meaningful. Because we found the AO/QBO interaction to be highly significant at 2 and 3 hPa, these effects ought to be present in a time series of NCEP temperatures for the midlatitude upper stratosphere, too.

4.5. Solar Cycle and Trend Terms

[26] It is reasonable to expect a solar cycle (SC) effect in middle atmosphere temperature, so we also checked to see if we could fit a 4015-day (11-year) SC term to the residual. This term is 99% significant in the upper mesosphere (Table 1) with an amplitude ranging from 1.0 to 1.7 K. Its maximum occurs from mid-1992 to mid-1993 (Table 2) or several years after solar maximum, which may be why our regression against the time series of the F10.7 cm solar flux did not show an equivalent relation. The effect of the SC and the IA terms shows up clearly in Figure 1f.

[27] Long-term cooling trends have been reported for the middle atmosphere for the late 1960s and into the 1990s [e.g., *Ramaswamy et al.*, 2001]. *Akmaev and Fomichev* [2000] have estimated cooling trends due to increases of CO_2 to be of the order of 0.8 K per decade. A periodic term corresponding to the length of the data can be an indication of unaccounted for polynomial trend terms. But when we considered those polynomial terms, they did not lead to a more acceptable model. For example, linear trend terms were introduced into the MLR model for upper levels of the stratosphere. They were significant at the 65% to 70% level and indicated a cooling of ~0.8 K over the 9.5 years of data. Although this amount of cooling is reasonable, we also found that the inclusion of the linear term caused the previous IA terms to become much less significant. In the upper mesosphere the linear term had little effect on the significant SC and IA terms, and, in fact, was not even marginally important. Because our rule of thumb in this analysis was to include only the model terms that were highly significant, we did not find significant cooling trends at any level for the HALOE time series of 40°N.

5. Results at Other Latitudes

5.1. SS/SR Differences and Seasonal Cycles

[28] Figure 2 and Table 3 show the SS minus SR values as a function of latitude zone. Maximum positive differences of ~3 to 4 K occur near 1 hPa at midlatitudes in both hemispheres. In the mesosphere the tidal phases at a pressure level change somewhat with latitude but are symmetric about the tropics. At 40° latitude of both hemispheres the apparent vertical wavelength for the tidal variations is ~32 km. Because the tropical zone is fairly wide, the signature of its tidal effects is an average across that zone, as shown in Figure 2. SS/SR differences are near zero in the upper tropical stratosphere but increase to 5.7 K at 0.1 hPa, primarily in response to the diurnal tide.

[29] The amplitudes and day of maximum for the AO cycles are given in Table 4 and Figure 3 as a function of latitude and altitude. Phases in Figure 3 are given as month of the year for the maximum, where the value of 1.0 represents 15 January and 12.0 is 15 December (the range for the year being 0.5 to 12.5 in order to be compatible with a similar phase plot for the CIRA reference atmosphere) [*Fleming et al.*, 1990, Figure 5.2]. To avoid the appearance of a discontinuity when the phase crosses from 12.5 to 0.5, we also allowed the phase to go to zero and negative. Thus 15 December may also be labeled as 0.0, 15 November as −1.0, etc., and those negative contours are dashed. At ~30° to 40° latitude of each hemisphere, there is a near-AO phase reversal with altitude at ~0.15 hPa. Largest AO amplitudes occur at 40° latitude in the upper stratosphere and the upper mesosphere. We find good seasonal symmetry for the NH and Southern Hemisphere (SH) middle latitudes, although the AO amplitudes are smaller in the upper stratosphere at 40°N than at 40°S. At 20° and 30° latitude the AO

Table 3. HALOE Sunset Minus Sunrise Temperature in K

P	40S	30S	20S	Eq	20N	30N	40N
5	−0.4	0.0	−0.1	0.0	0.3	0.3	−0.3
3	0.7	1.0	0.4	0.0	0.7	1.5	1.0
2	2.3	2.3	0.8	−0.1	1.3	2.7	2.7
1	3.4	3.5	2.8	0.4	3.4	4.0	4.2
0.5	1.6	2.8	2.6	2.5	2.5	3.2	3.0
0.3	0.0	1.4	1.9	4.2	1.6	1.4	1.2
0.2	−1.5	0.1	1.7	5.2	1.5	−0.3	−0.4
0.1	−2.6	−2.1	1.7	5.7	1.7	−0.8	−2.5
0.05	−1.1	−2.0	1.1	2.9	0.5	−1.0	−1.8
0.03	0.5	0.2	−0.2	−1.5	−0.6	0.6	0.3
0.02	2.3	2.3	−0.6	−5.2	−0.4	2.0	2.1
0.01	3.9	4.8	1.5	−6.2	1.2	3.5	3.8

Table 4. HALOE Annual Cycle Temperature Amplitude (Left Half) and Day of Maximum (Right Half)[a]

P	40S	30S	20S	Eq	20N	30N	40N	/40S	30S	20S	Eq	20N	30N	40N
5	9.2	3.5	0.7	0.7	1.5	2.1	4.5	357	352	287	109	126	138	151
3	8.6	5.3	1.9	0.8	1.2	3.4	5.9	355	351	348	110	109	137	153
2	9.5	6.0	1.9	1.0	1.3	3.1	6.1	355	350	345	117	122	142	154
1	8.0	3.6	0.9	*0.3	0.5	1.6	5.4	354	345	3	*344	44	141	157
0.5	6.7	2.7	0.9	2.3	0.6	1.7	5.3	354	353	12	30	27	169	166
0.3	4.9	2.0	1.1	2.2	0.7	*1.2	3.4	354	3	17	18	26	*181	168
0.2	2.4	1.5	1.4	2.2	*0.8	*0.5	1.6	349	13	20	14	*1	*246	169
0.1	1.6	0.9	2.2	2.5	2.3	1.8	2.0	177	66	24	14	5	338	1
0.05	4.9	*1.0	2.3	2.5	3.6	4.3	6.1	175	*67	11	10	19	13	5
0.03	6.6	*0.6	*1.8	*2.2	3.8	6.2	7.9	178	*62	*7	*349	21	23	9
0.02	7.2	0.8	*1.3	2.1	3.7	6.1	9.6	180	169	*9	323	15	18	12
0.01	9.6	*4.0	*0.5	*0.9	4.3	8.3	12.7	184	*186	*341	*350	11	8	10

[a] Terms denoted by an asterisk do not exceed 95% CI.

amplitude is larger in the NH than the SH for the upper mesosphere, but the opposite is true for the upper stratosphere and lower mesosphere. In other words, the seasonal cycle is not hemispherically similar for the subtropics. We suggest that this difference is a consequence of differences in the planetary and gravity wave forcing at midlatitudes of the two hemispheres. We note that in the upper mesosphere the June/December temperature differences are nearly zero at 30°S but of order 10 K at 30°N, most likely the result of the greater wintertime wave activity at the upper altitudes of the NH. Overall, there is very good continuity in the AO amplitudes and phases with pressure-altitude and for adjacent latitudes. The AO temperature maxima for NH and SH are also out-of-phase at middle latitudes by ~6 months, as expected.

[30] The amplitude and time of maximum for the SAO cycle are given in Table 5 and Figure 4. Phase information in Figure 4 is restricted to the month of occurrence for the temperature maximum from the first SAO cycle from January through June, where 15 January is 1.0, 15 June is 6.0 months. Phase discontinuities from December to January have been avoided by assigning a value of 0.0 to 15 December rather than 6.0. One can see that there is good continuity in the descent of the temperature maximum at all latitudes. The SAO has nearly the same phase at 20° and 30° latitude of the NH and SH, indicating a symmetric extension of its effects from tropical latitudes. The SAO amplitudes reach 6 K in the tropical upper mesosphere, decreasing to ~2 K in the stratosphere. The SAO term is not highly significant at some levels of the midlatitude NH upper stratosphere. Comparisons with the SAO cycle from CIRA [*Fleming et al.*, 1990, Figure 5.3] indicate significant differences in both its phase and amplitude, particularly at the lower latitudes. Part of the difference may be due to the fact that the HALOE SAO term is derived from its rather wide latitude bin centered at the equator. However, it is more likely that the large differences between the respective SAO amplitudes of the upper tropical mesosphere are a result of the much lower vertical resolution for the CIRA PMR data set at those pressure-altitudes, and possibly to S/N constraints in the retrieval of the PMR profile at its upper altitudes. An SAO cycle is the dominant periodic term in the HALOE MLR models for that region.

5.2. Interannual Terms

[31] The left half of Table 6 contains the IA amplitudes for just the upper stratosphere. Pressure-altitude rows with an asterisk indicate results for the 688-day cycle; entries for the other rows are for the nominal 800-day QBO cycle. Phase information is given on the right side of Table 6 in terms of the time for the maximum temperature in days since the beginning of its cycle. The IA phases change with latitude, but they exhibit good continuity in each hemisphere. We note that an 800-day, QBO-like term was also highly significant at 0.03 and 0.02 hPa at 40°S and at 0.3 hPa at 30°N, and that term was included in the final MLR models for those regions. Although IA processes must be acting throughout the mesosphere, they were left out of the

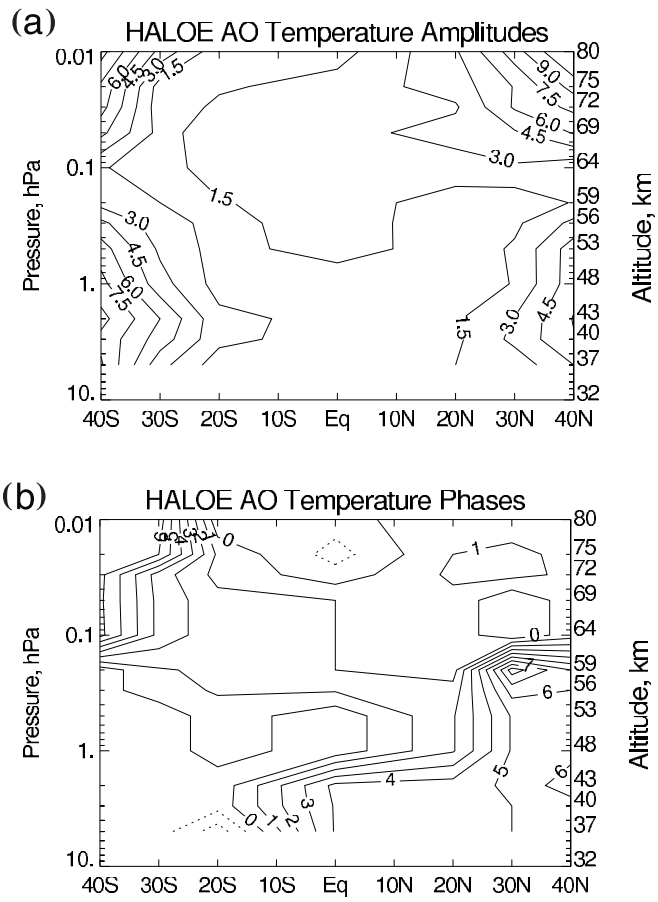

Figure 3. Annual temperature cycle from HALOE. (a) Amplitude (1.5 K interval). (b) Phase (month of the year for maximum; see text). Altitude scale is approximate.

Table 5. HALOE Semiannual Cycle Temperature Amplitude (Left Half) and Day of Maximum (Right Half)[a]

P	40S	30S	20S	Eq	20N	30N	40N	/40S	30S	20S	Eq	20N	30N	40N
5	1.6	*0.4	1.0	2.4	1.3	*0.4	*0.7	37	*36	101	107	108	*125	*180
3	1.4	0.5	1.0	2.8	1.1	0.3	0.8	35	40	102	103	103	157	180
2	1.3	*0.6	0.8	2.8	0.8	*0.4	1.0	25	*21	111	101	105	*4	180
1	*0.7	0.9	0.9	2.6	1.3	0.9	1.0	*178	149	103	79	100	126	135
0.5	1.7	1.5	1.3	1.0	1.8	2.1	2.5	15	126	94	55	75	109	125
0.3	2.6	2.2	1.5	0.9	1.8	2.7	3.4	142	116	78	41	63	103	118
0.2	3.0	2.6	1.3	1.3	1.5	2.6	4.4	134	114	71	43	69	109	113
0.1	3.7	2.2	1.0	3.1	1.7	2.1	5.0	118	112	46	37	27	107	108
0.05	3.5	1.9	2.5	5.9	3.4	2.5	4.0	106	100	25	25	26	57	88
0.03	2.8	1.9	3.8	6.4	4.4	4.0	3.4	90	54	22	11	20	43	67
0.02	2.8	2.6	3.9	5.7	4.1	4.0	3.4	74	42	17	1	14	33	52
0.01	2.4	1.5	1.9	2.7	2.0	3.1	*3.0	64	10	5	167	5	24	*40

[a] Terms denoted by an asterisk do not exceed 95% CI.

final models for most levels because they did not meet the 95% CI threshold criterion.

[32] There is a significant, subbiennial cycle due to the interaction of the AO and QBO cycles at both 30°N and 40°N at 3 hPa. The subbiennial (688-day) and the 800-day terms are nearly out-of-phase. Because each of these terms shows reasonable continuity with latitude and altitude, they are considered physically meaningful. Subbiennial terms are also present at 5 hPa at 30°N and at 2 hPa at 40°N, although their phases are not the same. However, at 30°S and 3 hPa both IA terms are nearly in phase. IA-term comparisons between 30°N and 30°S indicate that the QBO (800-day) term is symmetric, while the AO/QBO (688-day) term is antisymmetric. Similar results were reported by *Randel et al.* [1998] and *Dunkerton* [2001] from time series of the HALOE-observed species profiles. The nominal (800-day) QBO cycle is the only significant IA term at low latitudes.

[33] *Dunkerton* [2001] predicted that the AO/QBO species interaction would be most pronounced in the NH subtropics. Amplitudes for our IA terms are also larger in the NH. Most importantly, there is continuity of phase for this interaction in the upper stratosphere at 40°N and 30°N, indicating that these model terms are physically realistic. Such interactions within the upper stratosphere have also been shown to be important for a successful simulation of the effects of the QBO on interannual variations in the meridional transport across the subtropics [e.g., *Gray et al.*, 2001].

5.3. Solar Cycle and Linear Trend Terms

[34] Table 7 summarizes the occurrence of the SC and linear (*) terms in the HALOE data set. Neither term is present at 40°S, so that latitude is not shown. Significant SC terms were found in the upper stratosphere for the tropics and at 20°N. The date in Table 7 for its maximum stratospheric value (in years since 1 January 1991) occurs around 2000/2001 and is generally in phase with the solar cycle, as defined by the time series of the 10.7 cm energy flux. Similar SC terms are also found at 0.2 and 0.3 hPa at 30°S. In each case the SC amplitude is of order 0.4 K. The only anomalous term is at 5 hPa at 30°S; it is nearly out-of-phase with the SC.

[35] Periodic (11-year) terms are also present in the upper mesosphere at 20°N, 30°N, 40°N, 20°S, and 30°S. Their amplitudes are larger and range from 0.7 K to 2 K, but their peak values occur in late 1991 to mid-1993, a year or so after solar maximum. Although it is difficult to determine the exact SC phase from just 9.5 years of data, perhaps we are seeing a delayed and indirect response from the refocussing of planetary wave activity brought about by the SC effects on the production of ozone in the upper stratosphere. The pronounced occurrence of the SC at northern middle latitudes is consistent with the fact that wave activity is greater in the NH. Alternatively, the response may be caused by a decadal-scale interaction of the SC with the QBO zonal wind cycle of the stratosphere [*Salby and Callaghan*, 2000; *Soukharev and Hood*, 2001; *Shindell et*

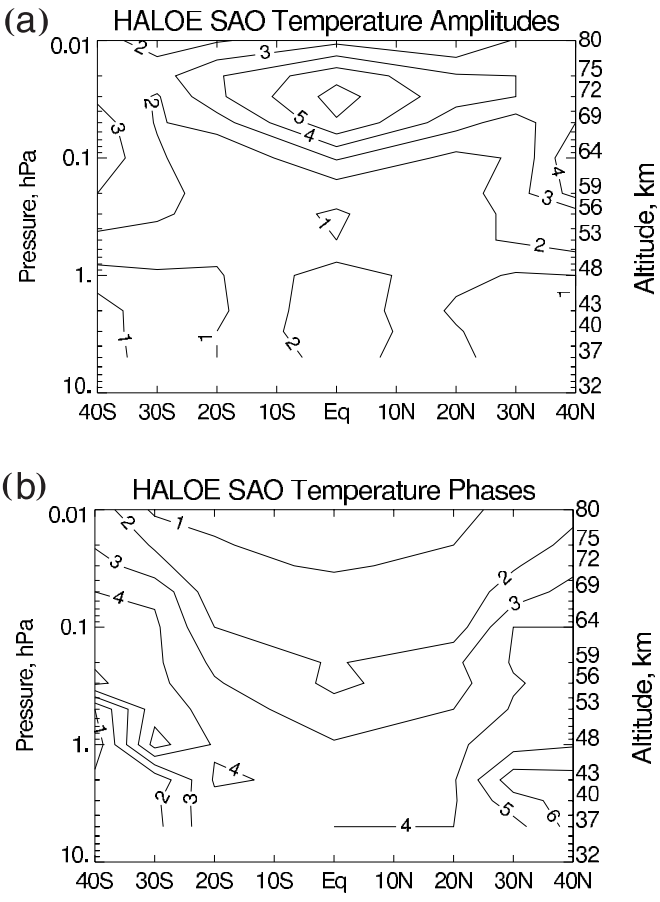

Figure 4. Semiannual temperature cycle from HALOE. (a) Amplitude (1.0 K interval). (b) Phase (month of year for first SAO cycle maximum; see text). Altitude scale is approximate.

Table 6. HALOE Interannual Cycle Temperature Amplitude (Left Half) and Day of Maximum (Right Half)[a]

P	40S	30S	20S	Eq	20N	30N	40N	/40S	30S	20S	Eq	20N	30N	40N
5*	–	–	–	–	–	0.4	–	–	–	–	–	–	145	–
3*	–	0.3	–	–	–	0.5	0.7	–	528	–	–	–	160	191
2*	–	–	–	–	–	–	0.7	–	–	–	–	–	–	209
5	0.7	–	–	0.7	–	–	0.8	647	–	–	216	–	–	586
3	0.8	0.6	0.3	1.0	–	1.0	0.9	620	566	306	170	–	436	540
2	0.9	0.5	0.4	0.6	0.6	0.7	0.9	603	489	268	113	275	504	506
1	–	–	–	–	0.5	0.6	0.7	–	–	–	–	221	301	467

[a] Top three rows of table (with asterisk) are for 688-day interannual cycle; bottom four rows are for 800-day cycle.

al., 1999]. It is also possible that there was a perturbation in the wave forcing of the net circulation in the mesosphere in 1991/1992 due to the radiative effects on the stratosphere from the volcanic aerosols of Mount Pinatubo. That event may have altered the timing of the maximum for the SC term in the early 1990s [*Rind et al.*, 1992]. Whatever the exact forcing mechanism, our SC-like term exhibits good continuity in the NH upper mesosphere.

[36] Linear terms are indicated in Table 7 with an asterisk. We found a significant (95% CI) and realistic linear cooling trend at 0.3 and 0.2 hPa at 20°N. That cooling is between 1.0 K and 1.6 K over 9.5 years, or 0.10 to 0.16 K per year. The cooling of 1.2 K at 1 hPa in the tropics is really the net difference of the coefficients of a linear and a quadratic term in its model. A separate model with only the linear term has the equivalent coefficient but is less significant. These cooling rates are consistent with the model calculations of *Akmaev and Fomichev* [2000] for the observed increases in atmospheric CO_2.

6. Comparisons With Other Data Sets

[37] Table 8 and Figure 5 show the zonal mean distribution of the annual average temperature from HALOE, the sum $a + b\,T_{mean}$. The corresponding distribution from CIRA can be found in *Fleming et al.* [1990, their Figure 5.1]. Figure 6 is a plot of the HALOE-CIRA profiles for several latitudes from those distributions, and it is clear that there are large differences over the 20-year span between these two data sets. HALOE is cooler in the upper stratosphere, warmer in the midmesosphere, and then cooler in the upper mesosphere. We found similar differences at 40°N and at 40°S (not shown) when the comparisons were restricted to summer months, for example, December at 40°S and June at 40°N. This finding indicates that the differences of Figure 6 are not traceable to just those winter months when there were significant wave variations along a zone of latitude. It is also not likely that the differences are due to interannual or solar cycle effects, based on the amplitudes of those effects from our analyses of the HALOE time series. Furthermore, the profile difference pattern in the mesosphere is not what one would expect from the radiative effects from the trends of CO_2.

[38] *Clancy et al.* [1994] reported differences between their SME climatology and CIRA that are similar to those of HALOE and CIRA in Figure 6. On the other hand, they found better agreement in the vertical variations of monthly average profiles from SME, sounding rockets, lidar, and the Stratospheric and Mesospheric Sounder (SAMS) data set, all of which were for the early 1980s. *Leblanc et al.* [1998, their Plate 2] also report similar differences for their seasonal lidar comparisons versus CIRA at middle and low latitudes. Our HALOE comparisons with nearly coincident lidar and falling sphere profiles exhibit no clear bias except perhaps near the mesopause [*Remsberg et al.*, 2002]. More exact comparisons between the HALOE and SME climatologies must be made in altitude space, which means that the HALOE time series analyses would have to be repeated for constant altitude rather than pressure levels, and we have not done that. However, the periodic seasonal terms (AO and SAO) from the HALOE MLR model have been combined with the constant and autoregressive terms from Table 8 to generate the seasonal HALOE "climatology" of middle atmosphere temperature at 40°N as shown in Figure 7. That HALOE result agrees well with the local lidar station climatologies obtained from the mid-1980s to the mid-1990s near 40°N,

Table 7. HALOE Solar Cycle (SC) Temperature Amplitude or Linear Coefficient (Left Half) and Time of Maximum of SC (Right Half)[a]

P	30S	20S	Eq	20N	30N	40N	/30S	20S	Eq	20N	30N	40N
5	0.5	–	0.5	0.5	–	–	6.2	–	8.6	8.7	–	–
3	–	–	0.3	–	–	–	–	–	9.3	–	–	–
2	–	–	–	0.4	–	–	–	–	–	9.9	–	–
1	–	–	−1.2*	0.5	–	–	–	–	*	9.6	–	–
0.5	–	–	–	–	–	–	–	–	–	–	–	–
0.3	0.4	–	–	−1.0*	–	–	10.3	–	–	*	–	–
0.2	0.4	–	–	−1.6*	–	–	10.2	–	–	*	–	–
0.1	0.7	–	–	–	–	–	0.9	–	–	–	–	–
0.05	1.3	–	–	–	–	1.0	0.9	–	–	–	–	2.3
0.03	–	1.2	–	–	1.9	1.5	–	1.8	–	–	1.6	1.9
0.02	–	1.2	–	1.2	2.0	1.7	–	1.8	–	1.6	1.5	1.5
0.01	–	–	–	0.7	1.8	–	–	–	–	0.9	0.9	–

[a] SC time of maximum is in terms of years since 1 January 1991; coefficient of linear term is indicated by asterisk and is in units of K per 9.5 years.

Table 8. HALOE Annual Average Temperature Distribution

P	40S	30S	20S	Eq	20N	30N	40N
5	238.4	240.9	242.3	243.2	242.4	241.1	239.5
3	246.8	249.4	250.9	251.8	251.3	250.7	248.9
2	253.8	257.0	258.4	259.3	258.9	258.0	256.3
1	259.4	262.2	264.6	267.3	264.5	262.5	261.1
0.5	254.3	256.0	258.3	261.1	258.3	255.9	255.7
0.3	247.2	248.0	250.0	252.9	251.3	248.0	248.1
0.2	240.5	240.5	242.1	244.4	244.0	241.2	240.9
0.1	226.9	226.4	226.4	225.5	226.7	227.0	226.8
0.05	213.4	211.7	210.3	206.4	210.0	211.9	212.6
0.03	205.3	202.4	200.4	197.4	199.8	202.5	204.4
0.02	201.2	197.8	196.1	194.7	195.1	197.7	199.8
0.01	196.9	196.5	193.9	193.2	192.1	193.8	194.8

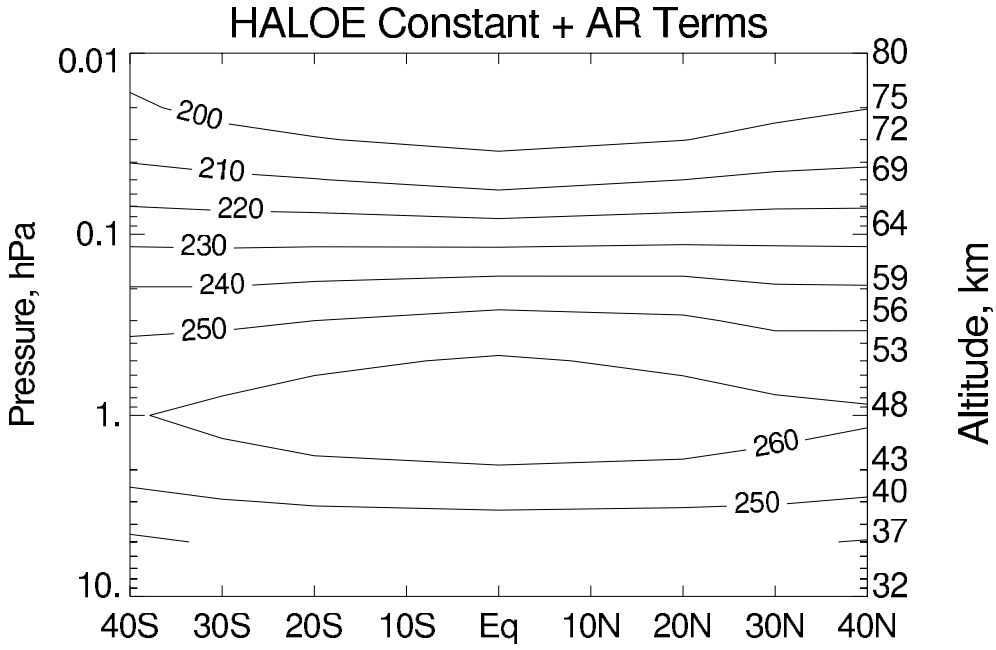

Figure 5. Annual, zonal average temperature distribution from HALOE.

as shown by *Leblanc et al.* [1998, their Plate 1]. Tabular monthly HALOE profiles can also be generated from the analyzed model terms at our other latitude zones. It is likely that the HALOE-CIRA patterns in Figure 6 for the mesosphere are a result of the much different measurement vertical resolutions for the two data sets and perhaps of the specific way in which the true radiance profiles were smoothed by the several PMR channels and then retrieved to yield temperature. It is also possible that slight biases arose when the PMR and SCR temperatures were merged to obtain the profile segment from ~40 to 56 km for the CIRA reference model [*Fleming et al.*, 1990].

[39] The CIRA climatology for the upper stratosphere is based mainly on the SCR measurements from Nimbus 5 and is likely more accurate than that from the PMR because of its better vertical resolution (~12 km) and better radiance signal-to-noise. That upper stratospheric part of CIRA also compares better with the profiles from SME and the correlative rocket and lidar data sets. Thus the HALOE-CIRA differences in Figure 6 for that region may be a good estimate of temperature change for the period of the mid-1970s to the mid-1990s. That change is of order 2.5 K per decade, much larger than that expected from the increases of CO_2 alone and larger than the linear trend term that we diagnosed from the HALOE time series for the decade of the 1990s. However, that larger change is consistent with the estimates of stratospheric cooling from other observations from 1979 to 1994 [*Ramaswamy et al.*, 2001].

7. Conclusions

[40] We determined the seasonal variations in the 9.5-year time series of the zonally averaged HALOE temperature profiles at latitude zones from 40°S to 40°N and at pressure-altitudes from 5 to 0.01 hPa. We resolved longer-period terms, too. In particular, we found evidence for weak (~0.8 K amplitude) QBO-like (800-day) variations at most latitudes of the upper stratosphere. Its phase changes with latitude but shows good symmetry across the NH and SH. We also resolved a significant subbiennial, 688-day cycle at subtropical latitudes. This cycle has been interpreted as the result of an interaction between the AO and QBO cycles; the subbiennial amplitudes are larger in the NH, most likely due to its greater wave activity. There is a solar cycle (SC) variation in the time series that is highly significant at some levels. Its amplitude is of the order of 0.5 K in the upper stratosphere to ~1.5 K in the upper mesosphere. However, the phase of this term changes with altitude in the middle

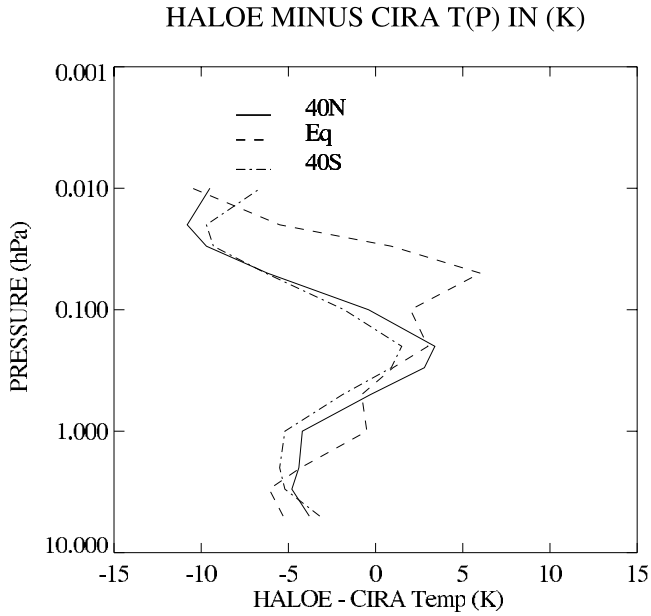

Figure 6. HALOE minus CIRA temperature profiles for 40°N, 40°S, and the equator.

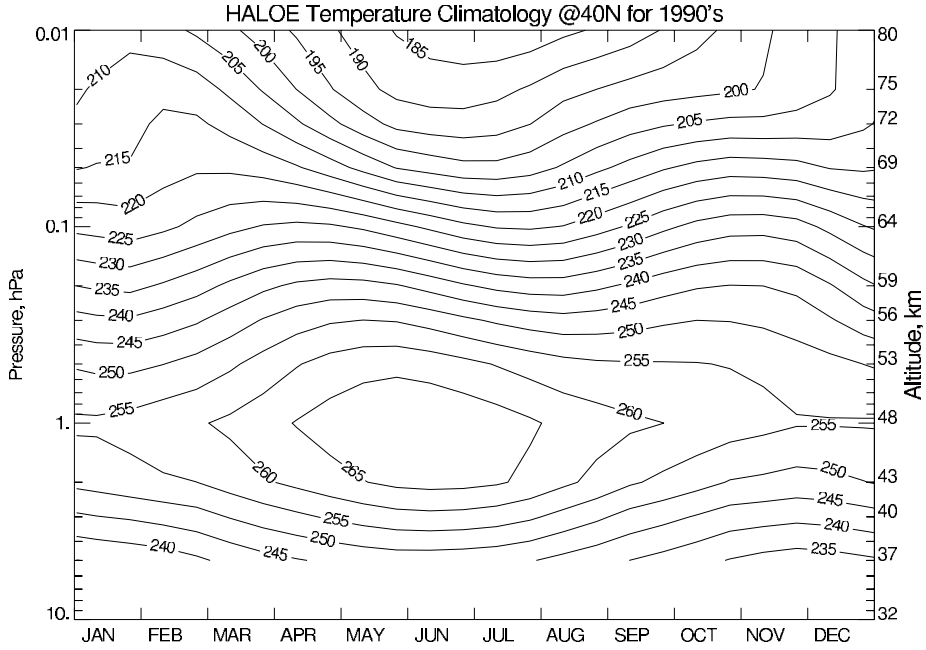

Figure 7. The zonal average seasonal temperature variation at 40°N from HALOE.

atmosphere, being in-phase with the solar cycle forcing in the upper stratosphere but delayed by several years in the upper mesosphere. We suggest that the mesospheric SC term is reflective of a decadal-type change in the effects of wave forcing on the net circulation of the mesosphere, perhaps induced by the solar forcing effects within the stratosphere.

[41] A significant cooling trend (1.0 to 1.6 K per decade) was found at 20°N in the midmesosphere and in the tropics at 1 hPa, where the cooling due to increases in CO_2 is expected to be of the order of 0.8 K per decade [*Akmaev and Fomichev*, 2000]. We found no highly significant stratospheric cooling for the 1990s at the other levels. We realize that this general finding of a weak cooling trend for the upper stratosphere is at odds with the larger trends reported from some other data sets. Yet, only the NCEP and lidar time series extend through the 1990s, and there has not been a published analysis of their trends for just that decade. Comparisons of the annual average temperatures from HALOE and CIRA indicate a cooling of the order of 2.5 K per decade for the upper stratosphere from the mid-1970s to the mid-1990s. Good estimates of the potential bias errors for each of those data sets must be provided to have confidence in that finding. *Akmaev and Fomichev* [2000] suggest that cooling trends of the 1970s and 1980s could be larger because of trends in other gases, such as the decline of upper stratospheric ozone due to the rapid rise of total chlorine plus the associated decrease in its heating of that region. Because total chlorine has leveled off in the mid to late 1990s [*Anderson et al.*, 2000], perhaps the decline of ozone at those altitudes has also slowed such that the HALOE temperature trends of the 1990s represent just the cooling due to the steady increase of CO_2. Obviously, more years of data are needed to know for sure, and it is important to continue the HALOE-like time series of middle atmosphere ozone and total chlorine for future decades to interpret any observed temperature trends.

[42] The relatively high, vertical resolution and the self-calibrating aspects of infrared, limb occultation experiments make them well suited for deriving the atmospheric temperature profile and for tying together the data time series from successive satellites. Because occultation measurements occur at local SR and SS, one can analyze for and remove most of the effects of the diurnal tide, which can complicate an interpretation of the variations in most other temperature time series of the middle atmosphere. We conclude that the sampling of a solar occultation experiment is adequate for determining highly significant, seasonal and longer period variations in the temperature. For these reasons the 9.5-year HALOE data set could be the basis of a more current seasonal temperature climatology for the upper stratosphere and mesosphere. We have also provided new observations about the significant hemispheric asymmetries in the AO and IA temperature cycles in the subtropics. Finally, we offer strong indications of solar cycle and perhaps other decadal-scale variations in middle atmosphere $T(p)$ that must be considered before a long-term cooling trend due to global increases in CO_2 or other gases can be certified from observations.

[43] **Acknowledgments.** The authors appreciate the insight that they gained from discussions with David Siskind and Tim Dunkerton on aspects of this work, as well as the anonymous comments from the reviewers. This study has been supported by UARS-related research funds administered by Mike Kurylo through NASA NRA-00-OES-09.

References

Akmaev, R. A., and V. I. Fomichev, A model estimate of cooling in the mesosphere and lower thermosphere due to the CO_2 increase over the last 3–4 decades, *Geophys. Res. Lett.*, *27*, 2113–2116, 2000.

Anderson, J., J. M. Russell III, S. Solomon, and L. E. Deaver, Halogen Occultation Experiment confirmation of stratospheric chlorine decreases in accordance with the Montreal Protocol, *J. Geophys. Res.*, *105*, 4483–4490, 2000.

Brasseur, G., The response of the middle atmosphere to long-term and short-term solar variability: A two-dimensional model, *J. Geophys. Res.*, *98*, 23,079–23,090, 1993.

Clancy, R. T., D. W. Rusch, and M. T. Callan, Temperature minima in the average thermal structure of the middle mesosphere (70–80 km) from analysis of 40- to 92-km SME global temperature profiles, *J. Geophys. Res.*, *99*, 19,001–19,020, 1994.

Considine, G. D., L. E. Deaver, E. E. Remsberg, and J. M. Russell III, Analysis of near-global trends and variability in Halogen Occultation Experiment HF and HCl data in the middle atmosphere, *J. Geophys. Res.*, *104*, 24,297–24,308, 1999.

Dudhia, A., S. E. Smith, A. R. Wood, and F. W. Taylor, Diurnal and semidiurnal temperature variability of the middle atmosphere, as observed by ISAMS, *Geophys. Res. Lett.*, *20*, 1251–1254, 1993.

Dunkerton, T. J., D. P. Delisi, and M. P. Baldwin, Middle atmosphere cooling trend in historical rocketsonde data, *Geophys. Res. Lett.*, *25*, 3371–3374, 1998.

Dunkerton, T. J., Quasi-biennial and subbiennial variations of stratospheric trace constituents derived from HALOE observations, *J. Atmos. Sci.*, *58*, 7–25, 2001.

Finger, F. G., M. E. Gelman, J. D. Wild, M. L. Chanin, A. Hauchecorne, and A. J. Miller, Evaluation of NMC upper-stratospheric temperature analyses using rocketsonde and lidar data, *Bull. Am. Meteorol. Soc.*, *24*, 789–799, 1993.

Fleming, E., S. Chandra, J. J. Barnett, and M. Corney, COSPAR International Reference Atmosphere, Chapter 2: Zonal mean temperature, pressure, zonal wind and geopotential height as a function of latitudes, *Adv. Space Res.*, *10*, 11–59, 1990.

Gaffen, D. J., Temporal inhomogeneities in radiosonde temperature records, *J. Geophys. Res.*, *99*, 3667–3676, 1994.

Garcia, R. R., S. Solomon, R. G. Roble, and D. W. Rusch, A numerical response of the middle atmosphere to the 11-year solar cycle, *Planet. Space Sci.*, *32*, 411–433, 1984.

Gray, L. J., E. F. Drysdale, T. J. Dunkerton, and B. N. Lawrence, Model studies of the interannual variability of the northern-hemisphere stratospheric winter circulation: The role of the quasi-biennial oscillation, *Q. J. R. Meteorol. Soc.*, *127*, 1413–1432, 2001.

Harris, N., R. Hudson, and C. Phillips (Eds.), Assessment of trends in the vertical distribution of ozone, *SPARC Rep. # 1*, 289 pp., World Meteorol. Org., Geneva, 1998.

Hervig, M. E., et al., Validation of temperature measurements from the Halogen Occultation Experiment, *J. Geophys. Res.*, *101*, 10,277–10,285, 1996.

Hitchman, M. H., and C. B. Leovy, Diurnal tide in the equatorial middle atmosphere as seen in LIMS temperatures, *J. Atmos. Sci.*, *42*, 557–561, 1985.

Huang, T. Y. W., and G. P. Brasseur, Effect of long-term solar variability in a two-dimensional interactive model of the middle atmosphere, *J. Geophys. Res.*, *98*, 20,413–20,427, 1993.

Huesmann, A. S., and M. H. Hitchman, The stratospheric quasi-biennial oscillation in the NCEP reanalyses: Climatological structures, *J. Geophys. Res.*, *106*, 11,859–11,874, 2001.

Keckhut, P., A. Hauchecorne, and M.-L. Chanin, Midlatitude long-term variability of the middle atmosphere: Trends and cyclic and episodic changes, *J. Geophys. Res.*, *100*, 18,887–18,897, 1995.

Keckhut, P., et al., Semidiurnal and diurnal temperature tides (30–55 km): Climatology and effect on UARS-Lidar data comparisons, *J. Geophys. Res.*, *101*, 10,299–10,310, 1996.

Keckhut, P., F. J. Schmidlin, A. Hauchecorne, and M.-L. Chanin, Stratospheric and mesospheric cooling trend estimates from U.S. rocketsondes at low-latitude stations (8°S–34°N), taking into account instrumental changes and natural variability, *J. Atmos. Sol. Terr. Phys.*, *61*, 447–449, 1999.

Keckhut, P., J. D. Wild, M. Gelman, A. J. Miller, and A. Hauchecorne, Investigations on long-term temperature changes in the upper stratosphere using lidar data and NCEP analyses, *J. Geophys. Res.*, *106*, 7937–7944, 2001.

Leblanc, T., I. S. McDermid, P. Keckhut, A. Hauchecorne, C. Y. She, and D. A. Krueger, Temperature climatology of the middle atmosphere from long-term lidar measurements at middle and low latitudes, *J. Geophys. Res.*, *104*, 17,191–17,204, 1998.

Lindzen, R. S., Thermally driven diurnal tide in the atmosphere, *Q. J. R. Meteorol. Soc.*, *93*, 18–42, 1967.

Luebken, F.-J., Nearly zero temperature trend in the polar summer mesosphere, *Geophys. Res. Lett.*, *21*, 3603–3606, 2000.

Ramaswamy, V., et al., Stratospheric temperature trends: Observations and model simulations, *Rev. Geophys.*, *39*, 71–122, 2001.

Randel, W. J., and F. Wu, Isolation of the ozone QBO in SAGE II data by singular value decomposition, *J. Atmos. Sci.*, *53*, 2546–2559, 1996.

Randel, W. J., F. Wu, J. M. Russell III, A. Roche, and J. W. Waters, Seasonal cycles and QBO variations in stratospheric CH_4 and H_2O observed in UARS HALOE data, *J. Atmos. Sci.*, *55*, 163–185, 1998.

Randel, W. J., F. Wu, J. M. Russell III, J. M. Zawodny, and J. Nash, Interannual changes in stratospheric constituents and global circulation derived from satellite data, in *Atmospheric Science Across the Stratopause*, *Geophys. Monogr. Ser.*, vol. 123, pp. 271–285, AGU, Washington, D. C., 2000.

Remsberg, E. E., P. P. Bhatt, and T. Miles, A comparison of Nimbus 7 limb infrared monitor of the stratosphere and radiosonde temperatures in the lower stratosphere poleward of 60°N, *J. Geophys. Res.*, *97*, 13,001–13,014, 1992.

Remsberg, E. E., P. P. Bhatt, and L. E. Deaver, Ozone changes in the lower stratosphere from the Halogen Occultation Experiment for 1991 through 1999, *J. Geophys. Res.*, *106*, 1639–1653, 2001.

Remsberg, E., et al., An assessment of the quality of Halogen Occultation Experiment temperature profiles in the mesosphere based on comparisons with Rayleigh backscatter lidar and inflatable falling sphere measurements, *J. Geophys. Res.*, *107*, doi:10.1029/2001JD001521, in press, 2002.

Rind, D., N. K. Balachandran, and R. Suozzo, Climate change and the middle atmosphere, Part II: The impact of volcanic aerosols, *J. Clim.*, *5*, 189–208, 1992.

Russell, J. M., III, et al., The Halogen Occultation Experiment, *J. Geophys. Res.*, *98*, 10,777–10,797, 1993.

Salby, M., and P. Callaghan, Connection between the solar cycle and the QBO: The missing link, *J. Clim.*, *13*, 2652–2662, 2000.

Scaife, A. A., J. Austin, N. Butchart, S. Pawson, M. Keil, J. Nash, and I. N. James, Seasonal and interannual variability of the stratosphere diagnosed from UKMO TOVS analyses, *Q. J. R. Meteorol. Soc.*, *126*, 2585–2604, 2000.

Shindell, D., D. Rind, N. Balachandran, J. Lean, and P. Lonergan, Solar cycle variability, ozone, and climate, *Science*, *284*, 305–308, 1999.

Soukharev, B. E., and L. L. Hood, Possible solar modulation of the equatorial quasi-biennial oscillation: Additional statistical evidence, *J. Geophys. Res.*, *106*, 14,855–14,868, 2001.

Wallace, J. M., R. L. Panetta, and J. Estberg, Representation of the equatorial stratospheric quasi-biennial oscillation in EOF phase space, *J. Atmos. Sci.*, *50*, 1751–1762, 1993.

Weatherhead, E. C., et al., Factors affecting the detection of trends: Statistical considerations and applications to environmental data, *J. Geophys. Res.*, *103*, 17,149–17,161, 1998.

World Meteorological Organization (WMO), Scientific assessment of ozone depletion: 1998, *Rep. # 44*, Geneva, Switzerland, 1999.

Zhu, X., J.-H. Yee, D. F. Strobel, X. Wang, and R. A. Greenwald, On the numerical modeling of middle atmosphere tides, *Q. J. R. Meteorol. Soc.*, *125*, 1825–1857, 1999.

P. P. Bhatt, SAIC, One Enterprise Parkway, Suite 300, Hampton, VA 23666, USA.

L. E. Deaver and E. E. Remsberg, NASA Langley Research Center, MS 401B, Hampton, VA 23681, USA. (e.e.remsberg@larc.nasa.gov)